



Investigating the performances of stepwise patched double lap joint

Wen-Yen Chuang, Jia-Lin Tsai *

Department of Mechanical Engineering, National Chiao Tung University, Hsinchu 300, Taiwan

ARTICLE INFO

Article history:

Accepted 21 December 2012

Available online 9 January 2013

Keywords:

Composites

Finite element stress analysis

Fatigue

Joint design

ABSTRACT

An adhesive-bonded double-lap composites joint with stepwise attachments was proposed and investigated experimentally and numerically in this study. For the conventional double lap joint (DLJ), the high shear stress and peel stress taking place in the adhesive layer near the patch termination significantly influenced the joint strength. In order to diminish the amount of the stresses, a new design of stepwise patch was introduced in the fabrication of the double-lap joint. Based on the finite element stress analysis (FEA), it was found that both shear stress and peel stress within the adhesive layer were reduced appreciably by the employment of the stepwise attachment. In addition, experimental results illustrated that the double lap joint with stepwise patch exhibited not only higher joint strength, but also it showed longer fatigue life than the conventional double lap joints.

© 2013 Elsevier Ltd. All rights reserved.

1. Introduction

Adhesive bonding has been an attractive method of joining composites' parts together because it can prevent the damage of the continuous fiber composites caused by mechanical fastening. Moreover, weight saving and corrosion resistances are also advantages of the adhesive joint over the traditional rivet and bolt joints. There are many different configurations of adhesive joints, among which the most commonly used are lap joints, i.e., single lap joint and double lap joint. This is because of the lap joints being quite simple and manufactured easily with low cost. However, the joint strength as well as the load carrying capacity of the lap joints are always significantly affected by the high peel stress and shear stress generated within the bonding layer. Therefore, the main design tasks of lap joints are toward the reduction/prevention of local stress concentration and the contribution of more uniform stress distribution as well.

Double lap joint (DLJ) without the attributes of eccentricity demonstrates higher strength than single lap joint [1,2]. Lee et al. [1] compared the joint strength of double lap joint and supported single lap joint, indicating that the double lap joint provides better performance than the single lap joint. A similar tendency was also observed by Taib et al. [2]. Choupani [3] characterized the effect of joint configuration as well as the adhesive thickness on the strength of the adhesively bonded double lap joints by means of the finite element analysis. Based on the fracture mechanics and the stress analysis in the bonding layer, the factors influencing the strain energy release rate and the stress

concentration in the double lap joint were discussed. The effects of temperature variation on the tensile strength of double lap joints were examined by Zhang et al. [4]. It was found that the failure mechanism changes from the fiber-tear to adhesive failure as the temperature increases. Sheppard et al. [5] introduced a damage zone model to predict the failure load of adhesively bonded joints. It was revealed that the model predictions achieve good correlation with the experimental data. Cheuk et al. [6] developed an analytical model to investigate the crack propagation behaviors in metal-to-metal double lap joint under fatigue loading. The energy release rate calculated based on their analytical model was correlated well with the finite element analysis. In addition, the mixed mode fatigue crack growth in double lap joints was characterized by Cheuk et al. [7] using the concept of equivalent strain energy release rate. Zhang et al. [8] investigated the crack initiation and propagation in double lap joints using a mixed mode fracture criterion associated with strain energy release rate expressed in the form of canonical elliptic equation. A comprehensive review of adhesively bonded joints in terms of finite element stress analysis and fracture analysis was provided by He [9]. In light of forgoing investigations, the stress distributions and the energy release rate of double lap joint associated with adhesive thickness and adhesive properties were mainly of concern; however, the novel design of the double lap joint for the improvement of joint strength and fatigue duration is scarce in literature. If a new design of double lap joint with notable performance can be accomplished, the adhesively bonded joint can be extensively employed in bonding the composite structures with reliability and safety.

In this study, the double lap joint with a new design of stepwise attachments was proposed and then validated by simple tensile tests and fatigue tests. Meanwhile, a 2-D finite element

* Corresponding author. Tel.: +886 3 5731608; fax: +886 3 5720634.
E-mail address: jialin@mail.nctu.edu.tw (J.-L. Tsai).

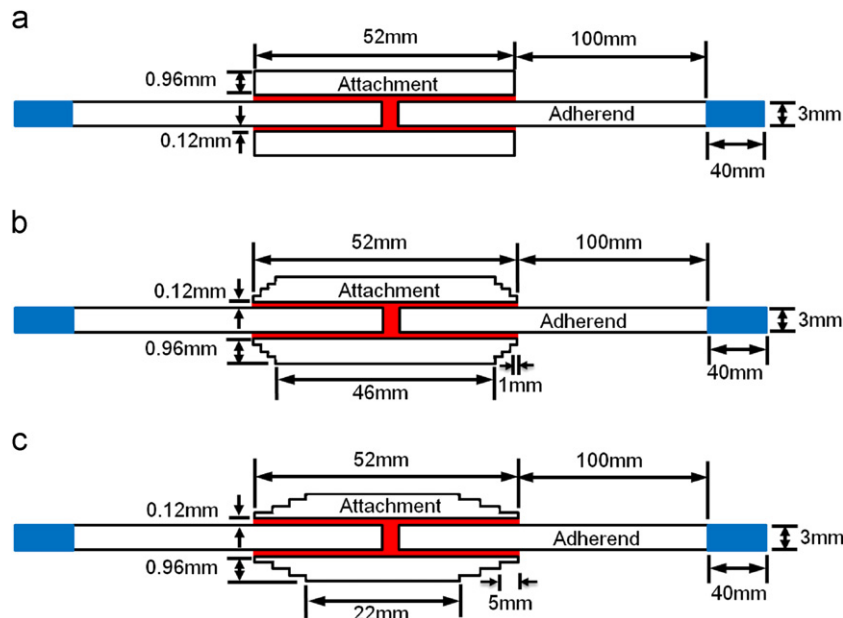


Fig. 1. Design of double lap joint: (a) conventional joint (DLJ), (b) stepwise patch joint (SDLJ-1) and (c) stepwise patch joint (SDLJ-2).

analysis was performed to elaborate the stress distribution as well as the energy release rate within the adhesive layer of the new design double lap joint. The numerical results correlated with the experimental data were utilized to elucidate the advantage of the stepwise attachment on the enhancement of the mechanical performance of the double lap joints.

2. Design of adhesive joint

The double lap joint with stepwise attachments was introduced and experimentally investigated. For reference purposes, the conventional double lap joint was also included in the investigation. The basic geometric configurations of the joints accounted for in the study are shown in Fig. 1. Fig. 1(a) indicates the conventional double lap joint, and for simplicity, it is denoted as DLJ. There are two different stepwise patched double lap joints in which the steps in the attachments are 1 mm and 5 mm respectively as shown in Fig. 1(b) and (c). These two stepwise joints are respectively indicated as SDLJ-1 and SDLJ-2. The gap between the two adherents in the joints is 2 mm, and the width of the samples is 25 mm. The bonding areas in the three joints are designed to be the same so that the effect of the attachment can be fully illustrated. The adherent was fabricated by graphite/epoxy composite laminates with the stacking sequence of $[0_2/90_2/0_3/90_2/0]_s$, and the attachment is made by graphite/epoxy unidirectional laminates of $[0]_8$. It is noted that in the description of the above layup sequence, the coordinate system is set coincided to the loading direction.

3. Fabrication and experiments

The fabrication of the double lap joints is described as follows. The unidirectional graphite/epoxy prepreg, provided by FTC Group Taiwan, was cut to the proper dimensions and then laid up manually in accordance with the designed stacking sequence. Autoclave curing was conducted on the laminates with the recommended curing process. The detail of curing cycle for the composite laminates is shown in Fig. 2. The adherents with the desired dimension were cut from the composites panels using a

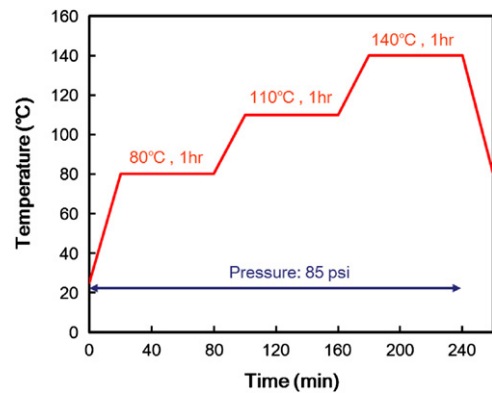


Fig. 2. Curing process of composite laminates.



Fig. 3. Photos of stepwise patch joint (SDLJ-2): (a) side view and (b) top view.

water jet. Similarly, the attachments for the DLJ samples were prepared from the 8-ply unidirectional composite panel. On the other hand, for the preparation of stepwise attachments, unidirectional prepreg was stacked layer by layer on a specially designed mold and then cured in the autoclave. It can be found that although the geometric configuration of stepwise attachment is not symmetric, the bonding surfaces of the stepwise attachment obtained from the molding process are quite flat. Subsequently, the adherents and the attachment were bonded together using epoxy adhesive and cured at 60 °C for 4 h. The thickness of the adhesive bonding line observed from the microscopy is around 0.12 mm. Afterward, a fiberglass end tab of 40 mm length was adhered to the specimens at both ends using epoxy glue. Fig. 3 illustrates the photos of the stepwise attached double lap joint. The material properties of graphite/epoxy composites

employed in the study are tabulated in Table 1. All properties were measured in our laboratory by following the ASTM standard 3039 [10] for tensile properties and ASTM standard 3518 [11] for in-plane shear properties. In addition to the mechanical properties of the composite laminates, the properties of the epoxy adhesive utilized to bond the attachments and adherents were also measured experimentally. Based on ASTM standard D638 [12], uniaxial tensile tests were conducted on the coupon specimens made of epoxy adhesive in stroke control mode. During the tensile tests, the stress and the corresponding strain were recorded and the constitutive relation is shown in Fig. 4. It can be seen that the nonlinear behavior of the epoxy adhesive is not substantial and the failure strain is less than 1%. It appears that this epoxy adhesive is brittle failure. The corresponding material constants of the adhesive epoxy obtained from tensile tests are summarized in Table 2.

In order to elaborate the effect of the stepwise attachment on the strength of DLJ, all specimens were tested to failure in tension. The experiments were conducted on a hydraulic MTS machine under stroke control at a displacement rate of 10^{-2} mm/s. During the tests, the displacement was measured directly from the linear variable differential transformer, and the loading histories were obtained from the load cell embedded on the loading fixture. Fig. 5 shows the typical load–displacement curve of the double lap joints. Basically, the rigidity of the double lap joints is almost the same and is not affected by the different types of attachments. For each case of double lap joints, five specimens were tested. Average strengths together with the standard deviation are shown in Fig. 6. Results revealed that the double lap joint (SDLJ-2) with 5 mm step attachments exhibits superior joint strength than others. Nevertheless, for the double lap joint with the attachments of 1 mm step (SDLJ-1), the strength is little less than that of the conventional double joint (DLJ), although the difference is within the experimental variation. For the SDLJ-1 samples,

Table 1
Material properties of graphite/epoxy composites.

Young's modulus		Poisson's ratio	Shear modulus
E_1 (GPa)	E_2 (GPa)	ν_{12}	G_{12} (GPa)
138	9.65	0.28	5.6

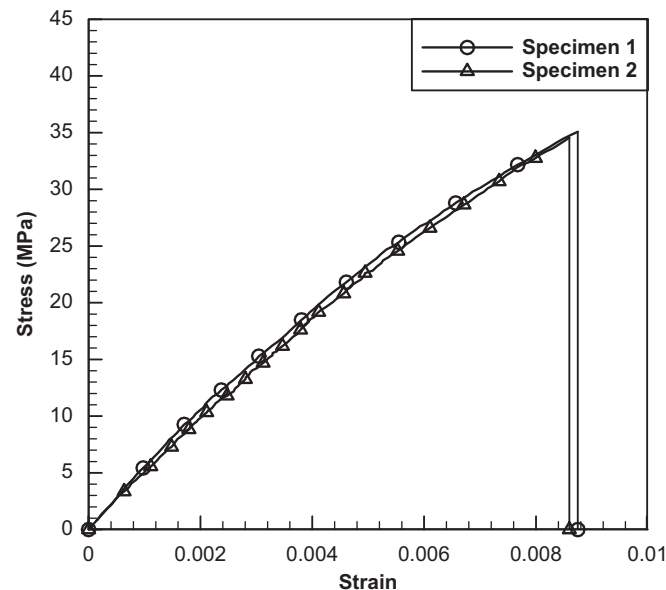


Fig. 4. Stress and strain curves of epoxy adhesive.

Table 2
Material properties of epoxy adhesive.

Tensile modulus E (GPa)	Poisson's ratio ν	Tensile strength S (MPa)
4.4	0.4	34.9

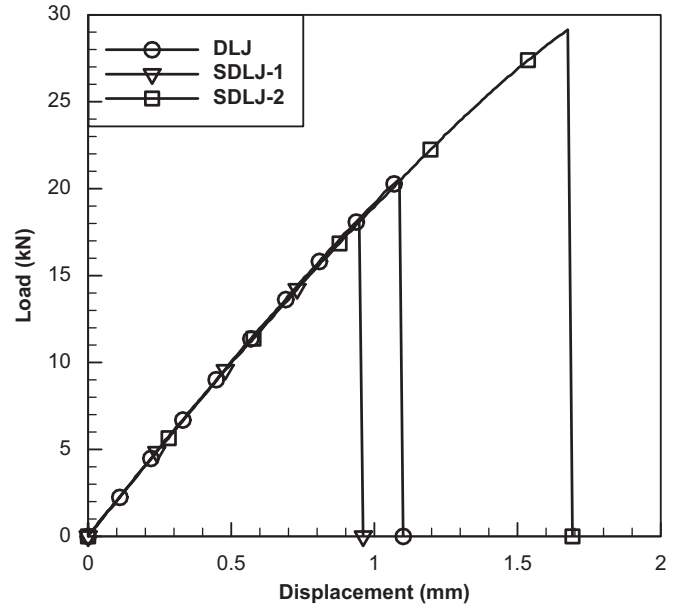


Fig. 5. Typical load–displacement curves for double lap joints under tensile tests.

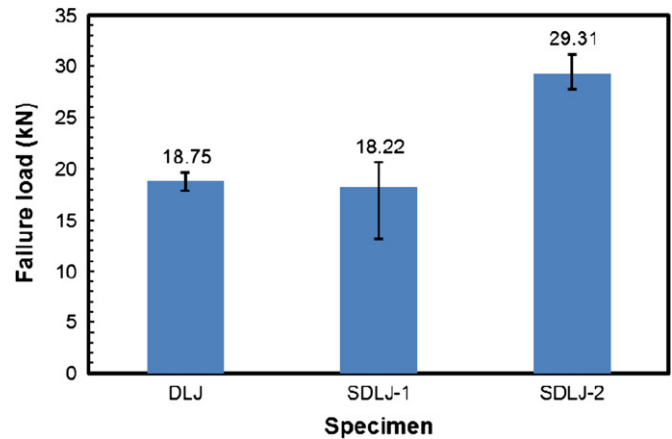


Fig. 6. Failure loads of the double lap joints.

because the steps in the attachment are only 1 mm, the contribution of the steps on the joint strength may not be substantial so that the strength is compatible to the traditional joint with the straight termination of attachments. On the contrary, for the SDLJ-2 samples, because the step in the attachments is 5 mm, the function of the stepwise attachment can be fully demonstrated, and the joint strength is around 50% higher than that of the conventional one. The failure surfaces of the stepwise double lap joints are shown in Fig. 7. It can be seen that there is clear epoxy adhesive left on the bonding surfaces of the attachment and adherent; therefore, the dominant failure mode can be recognized as the cohesive failure [13]. In other words, the failure of the adhesive joints is taking place within the bonding line of epoxy adhesive. With regard to why the attachment with 5 mm step can provide better joint strength than that with 1 mm step or straight

termination, we resort the assistance of finite element stress analysis to calculate the stress distribution within the adhesive bonding line.

4. Finite element stress analysis

In addition to the experiments, the superior performance of stepwise double lap joints was elucidated from the finite element stress analysis (FEA). Based on the geometric configuration of the specimens described earlier in Fig. 1, the finite element models for the three cases of double lap joints were generated respectively. Because of the attribute of symmetry, only a quarter of model, as shown in Fig. 8, was generated, and the constraint conditions with the displacement in either x or y directions being zero were imposed on the symmetric planes (as indicated by a dash line). The analysis was conducted with the commercial code ANSYS, and plane strain element (plane 182) was utilized to model the composites laminates (adherent and attachment) as well as the epoxy adhesive. It should be noted that the nonlinear geometric deformation was accounted for in the modeling, and

the materials were assumed to be linear elastic. Fig. 9 shows the mesh of the adhesive near the attachment termination. For the sake of comparison, the element size in the adhesive layer for the three cases was designated to be the same so that the relative amount of stress distribution can be justly demonstrated. The stress components along the middle line (x -axis) of the adhesive layer were calculated, and the values were normalized with respect to the applied loading. The comparison of the normalized peel stress distribution along the adhesive is shown in Fig. 10. Apparently, SDLJ-2 exhibits the lowest stress values as well as the most uniform stress distribution within the bonding line. In addition, the SDLJ-1 sample also demonstrates lower peel stress as compared to DLJ sample. Fig. 11 shows the shear stress distributions of the three lap joints. It can be seen that SDLJ-1 and DLJ almost have the same shear stress distribution as well as the peak values. However, SDLJ-2 specimen demonstrates the substantial reduction of shear stress distribution than the above two cases. Therefore, with the lower peel and shear stress distributions, it is not surprising that the SDLJ-2 specimen can have the better joint strength. However, for SDLJ-1, the stress can be reduced by the design of stepwise attachment, yet the deduction because of the 1 mm step is too little to compensate for the experimental variations resulting from the fabrication process and mechanical testing. This is the reason why SDLJ-1 has almost the same joint strength as DLJ.

The strengths of the double lap joints were then characterized using the damage zone model proposed by Sheppard et al. [5] together with the stress distributions obtained from the finite element analysis. It is noted that one of the advantages of using the damage zone mode is that the prediction results are not sensitive to the mesh size. Therefore, the calculated stresses based on the previous mesh configuration were directly utilized in the model predictions. Since the behavior of the epoxy adhesive is brittle, the failure of the adhesive joints is assessed based on the maximum principal stress criterion. The stress components of each element in the adhesive layer were calculated and then



Fig. 7. Failure surfaces of SDLJ-2 sample.

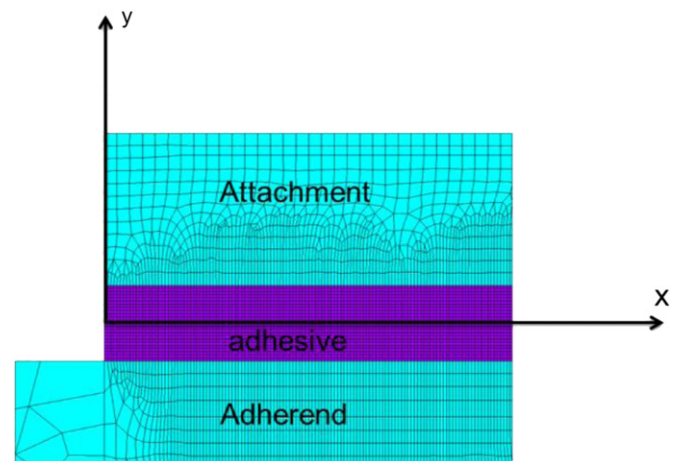


Fig. 9. Finite element meshes around the termination of adhesive.

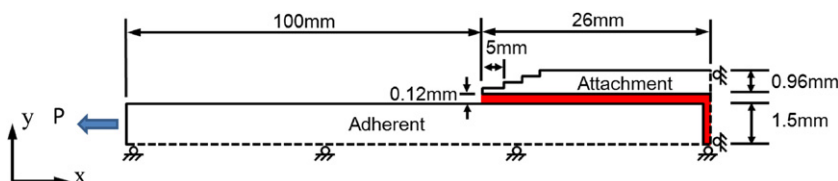


Fig. 8. A quarter model of double lap joint (SDLJ-2) in FEM analysis.

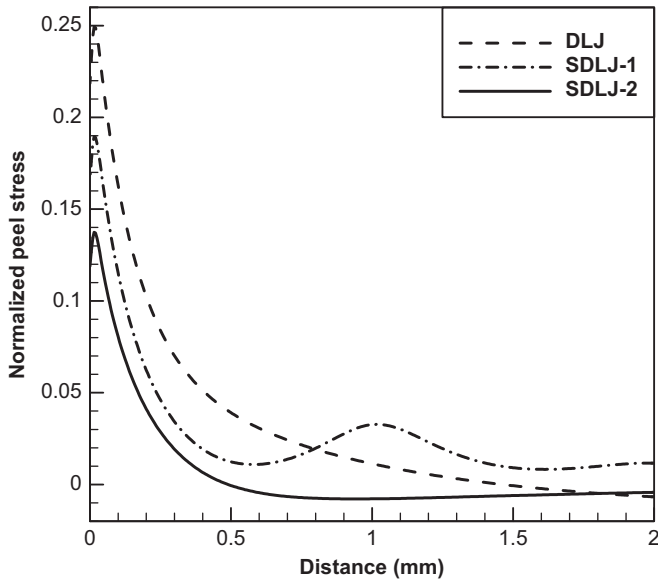


Fig. 10. Normalized peel stress distribution in the adhesive layer.

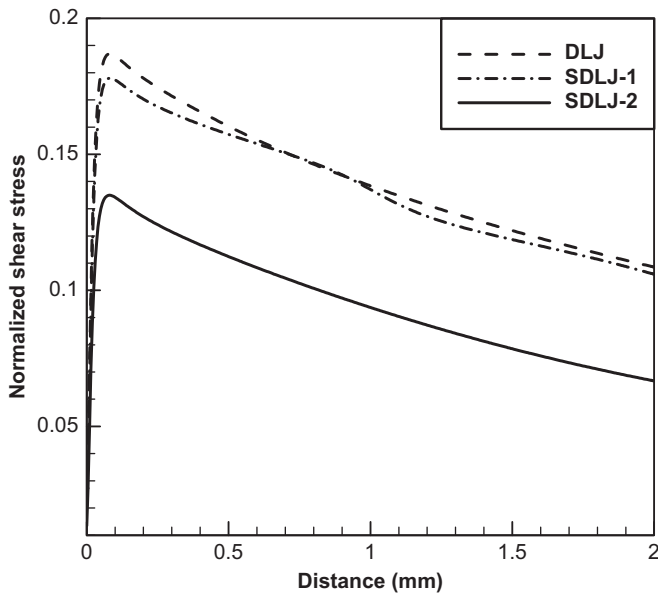


Fig. 11. Normalized shear stress distribution in the adhesive layer.

Table 3
Comparison of predicted failure load with experimental data.

Specimens	Experimental failure load (kN)			Predicted failure load (kN)	Ratio (FEA/Av. Exp.)
	Min.	Max.	Av.		
DLJ	13.62	21.16	18.75	21.15	1.13
SDLJ-1	16.69	20.06	18.22	19.94	1.09
SDLJ-2	26.05	33.7	29.31	26.4	0.90

transferred into the principal directions. When the principal stress of the element was larger than 34.9 MPa (tensile strength of epoxy adhesive), the area of the element was regarded as a damage zone. The summation of the damage area within the adhesive layer was utilized in the model predictions. The critical size of the damage zone was chosen so that the predicted values fall into the ranges of the experimental variations. The model

Table 4
Comparison of fatigue life for DLJ and SDLJ-2 samples.

P_{max}	DLJ (cycles)		SDLJ-2 (cycles)	
	9.5 kN	13 kN	9.5 kN	13 kN
6 Hz	260,086	9783	> 500,000	125,273
	135,325	8684	> 500,000	264,365
	108,182	8181	> 500,000	380,532
Avg.	167,864	8882	> 500,000	256,723
3 Hz	144,194	5390	> 500,000	51,526
	110,847	1997	> 500,000	79,447
	58,466	2280	> 500,000	22,608
Avg.	104,502	3222	> 500,000	51,193

predictions in terms of the critical damage zone size of 3.65 mm² are shown in Table 3 together with the experimental data. It can be seen that the predicted values for all joints are correlated to the average failure loads. Moreover, the superior performances of the SDLJ-2 with high joint strength are also illustrated in the damage zone model. For DLJ and SDLJ-1 joints, the predicted values are close to each other, which basically coincided with the experimental observations.

5. Fatigue tests

In addition to the joint strength, the fatigue performance of stepwise patched joint under cyclic loading was also examined. The fatigue tests were conducted in the hydraulic machine under two different loading frequencies (3 Hz and 6 Hz). Tensile–tensile sinusoidal loading with a load ratio $\sigma_{min}/\sigma_{max} = 0.1$ was applied on the joints. The maximum loads of P_{max} in the fatigue tests were designated to be 50% and 70% of the average joint strength of DLJ; therefore, the obtained values are 9.5 kN and 13 kN, respectively. Both the SDLJ-2 and DLJ samples were under the same cyclic loading condition, and the results are compared in Table 4. It can be seen that the SDLJ-2 reveals much longer fatigue life than DLJ in both cyclic frequencies of 3 Hz and 6 Hz. In addition, under different maximum loads, SDLJ-2 still illustrates longer fatigue duration. In light of the forgoing experiments, it is summarized that the stepwise joint (SDLJ-2) demonstrates not only higher joint strength but also longer fatigue duration, and then the new design can be employed to join the composites' components together with reliability.

From the observation of the fatigue failure specimens, it was found that the fracture took place within the epoxy adhesive. In general, the crack initiation and extension are the major failure mechanism during the fatigue loading. In an attempt to further understand the fatigue failure of the adhesive joints, the strain energy release rate of the fatigue crack initiated from the adhesive termination was investigated. It is noted that in our analysis, the crack was assumed to initiate from the adhesive termination and then extend along the mid-plane of the adhesive layer. The schematic of the quarter model with a crack embedded within the adhesive layer is shown in Fig. 12. The strain energy release rate was calculated using the crack closure technique [14] as

$$G_I = \lim_{\delta a \rightarrow 0} \frac{1}{2\delta a} f_y^b (u_y^a - u_y^a) \quad (1)$$

$$G_{II} = \lim_{\delta a \rightarrow 0} \frac{1}{2\delta a} f_x^b (u_x^a - u_x^a) \quad (2)$$

where G_I and G_{II} are the Mode I and Mode II strain energy release rate, respectively. f_x^b and f_y^b denotes the nodal force at node b in the

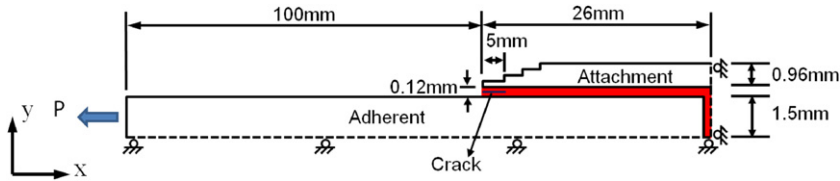


Fig. 12. A quarter model of double lap joint (SDLJ-2) with an embedded crack.

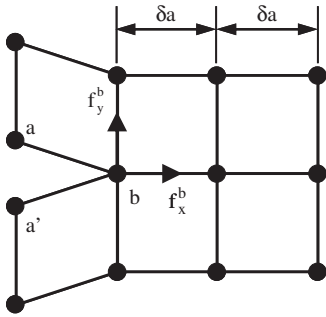


Fig. 13. Schematic of crack closure technique used in FEM analysis.

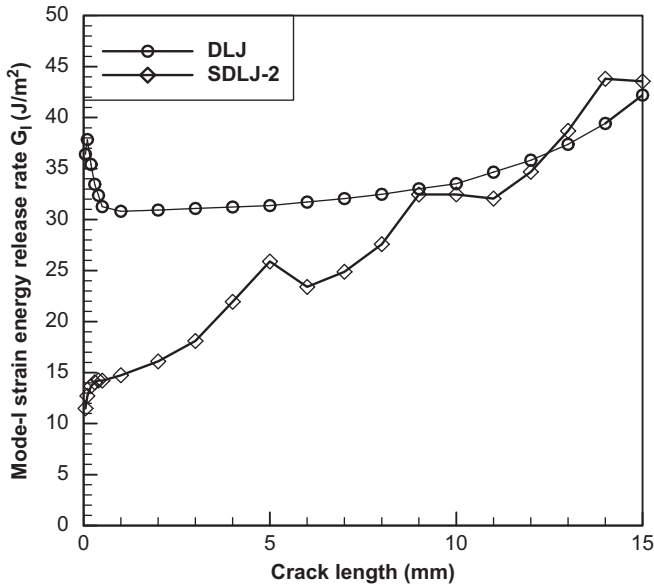


Fig. 14. Mode I strain energy release rates of SDLJ-2 and DLJ joints.

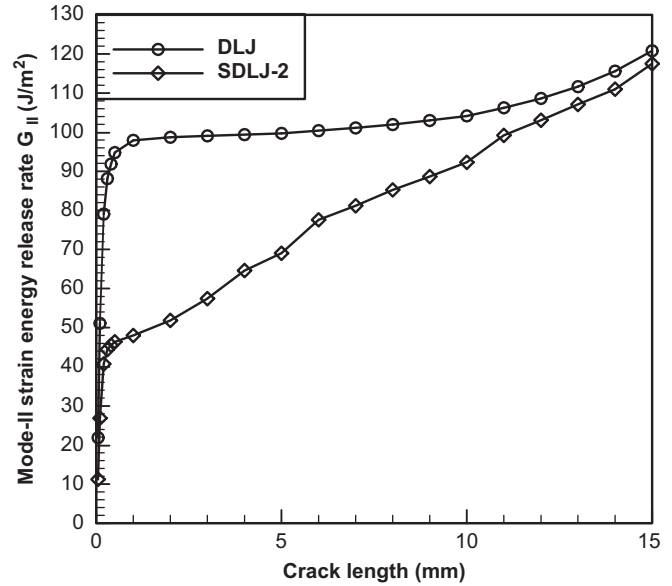


Fig. 15. Mode II strain energy release rates of SDLJ-2 and DLJ joints.

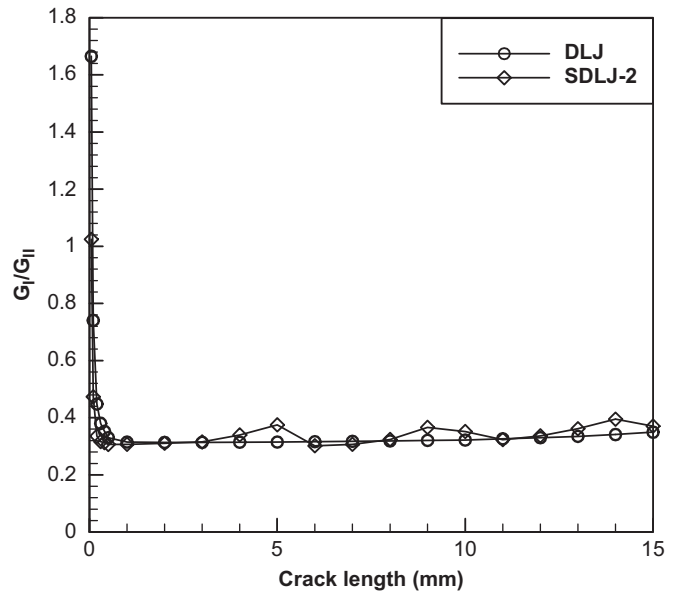


Fig. 16. Mode mixity of SDLJ-2 and DLJ joints.

x and y direction. u_x^a and u_y^a are the displacement components at node a, and $u_x^{a'}$ and $u_y^{a'}$ are the displacement components at node a' as illustrated in Fig. 13. In general, the FEM mesh near the crack tip should be fine enough to have a converged value of the strain energy release rate. In this study, the FEM mesh near the crack tip is designated as 0.5% of the crack length. The applied loading in the FEM analysis was 13 kN which is the maximum tensile load in the fatigue tests. Figs. 14 and 15 illustrate the variations of Mode I and Mode II strain energy release rate of the SDLJ-2 and DLJ joints along the crack extension. It can be seen that both Mode I and Mode II energy release rates in the SDLJ-2 are lower than those in the conventional DLJ. The low strain energy release rate indicates that the SDLJ-2 joint has better capability of retarding the crack onset and extension during the cyclic loading. This is the reason why SDLJ-2 can have longer fatigue duration. Due to the effect of the stepwise attachment, it was found that the SDLJ-2 depicts little wavy behavior in the Mode I energy release rate. Apparently, at the locations of the steps, i.e. 5 mm and 10 mm from the adhesive termination, the Mode I energy release rate moderately raises. On

the other hand, the Mode II energy release rate basically is not affected by the steps but monotonically increases as the crack length increases. The mode mixity of the fracture during the crack extension is shown in Fig. 16. Except near the adhesive termination, the value of Mode II energy release rate is greater than the Mode I value, which implies that the crack extension process is dominated by the Mode II fracture. In addition, the ratio of the mode mixity basically is not dramatically altered by the design of the attachment configuration.

According to the forgoing discussions, the superior property of stepwise joint can be appropriately elucidated from the two perspectives, stress analysis and fracture mechanics analysis. Associated with the same applied loading, it appears that the peel stress and shear stress in the adhesive layer of the stepwise joint are dramatically lower than those in the conventional joint. In other words, the employment of the stepwise attachment can effectively decrease the stress intensity in the adhesive layer resulting in the higher strength of the joint. Nevertheless, from the fracture mechanics viewpoint, it can be seen that the strain energy release rate of the stepwise joint is lower than that in the conventional joint. Obviously, the driving energy causing the crack extension in the stepwise joint is lower than that in the conventional joint and thus the fatigue durability of the stepwise joint can be longer.

6. Conclusions

Two new designs of stepwise attachments were proposed on the double lap joint, and the joint strength as well as the fatigue performance was investigated experimentally and numerically. Experimental observations validated that the double lap joint with the stepwise attachment of 5 mm steps demonstrates not only higher joint strength but also longer fatigue life. From the numerical simulation, it can be seen that when the designed step in the stepwise attachment is 5 mm, both the peel stress and shear stress within the double lap joint drop dramatically. On the other hand, when the step is only 1 mm, the reduction of shear stress is moderate such that the improvement of joint strength is limited. Based on the damage zone model, the joint strengths were predicted and good correlation with the experimental data was attained. The energy release rate of the adhesive joints with the crack extension was calculated using the crack closure

technique. It was found that the energy release rate in the SDLJ-2 is lower than that in the conventional DLJ. The low strain energy release rate indicates that the SDLJ-2 has better capability of retarding the crack onset under cyclic loading, resulting in long fatigue life.

References

- [1] Lee HK, Pyo SH, Kim BR. On joint strengths, peel stresses and failure modes in adhesively bonded double-strap and supported single-lap GFRP joints. *Compos Struct* 2009;87:44–54.
- [2] Taib AA, Boukhili R, Achiou S, Gordon S, Boukehili H. Bonded joints with composite adherends. Part I. Effect of specimen configuration, adhesive thickness, spew fillet and adherend stiffness on fracture. *Int J Adhes Adhes* 2006;26:226–36.
- [3] Choupani N. Characterization of fracture in adhesively bonded double-lap joints. *Int J Adhes Adhes* 2009;29:761–73.
- [4] Zhang Y, Vassilopoulos AP, Keller T. Effects of low and high temperatures on tensile behavior of adhesively-bonded GFRP joints. *Compos Struct* 2010;92:1631–9.
- [5] Sheppard A, Kelly D, Tong L. A damage zone model for the failure analysis of adhesively bonded joints. *Int J Adhes Adhes* 1998;18:385–400.
- [6] Cheuk PT, Tong L, Rider AN, Wang J. Analysis of energy release rate for fatigue cracked metal-to-metal double-lap shear joints. *Int J Adhes Adhes* 2005;25:181–91.
- [7] Cheuk PT, Tong L, Wang CH, Baker A, Chalkley P. Fatigue crack growth in adhesively bonded composite-metal double-lap joints. *Compos Struct* 2002;57:109–15.
- [8] Zhang Y, Vassilopoulos AP, Keller T. Mixed-mode fracture of adhesively-bonded pultruded composite lap joints. *Eng Fract Mech* 2010;77:2712–26.
- [9] He X. A review of finite element analysis of adhesively bonded joints. *Int J Adhes Adhes* 2011;31:248–64.
- [10] ASTM D3039. Standard test method for tensile properties of polymer matrix composite materials; 2008.
- [11] ASTM D3518. Standard test method for in-plane shear response of polymer matrix composite materials by tensile test of a $\pm 45^\circ$ laminate; 1995.
- [12] ASTM D638. Standard test method for tensile properties of plastics; 2003.
- [13] Ebnesajjad S. *Adhesives technology handbook*. 2nd ed. New York: William Andrew; 2008.
- [14] Sun CT, Jih CJ. On strain energy release rates for interfacial cracks in bi-material media. *Eng Fract Mech* 1987;28:13–20.